Zemin Mekaniği ve Geoteknik Mühendisliği
20. Ulusal Konferansı

15-16 Ekim 2026
Sakarya Üniversitesi

KOHEZYONLU-SÜRTÜNMELİ DOLGULU KONSOL İSTİNAT DUVARLARINDA AKTİF TOPRAK BASINCININ SAYISAL ANALİZİ

NUMERICAL ANALYSIS OF ACTIVE EARTH PRESSURE ON CANTILEVER WALLS IN COHESIVE-FRICTIONAL BACKFILL

Dina AQRA[1], Erol ŞADOĞLU[2]

ÖZET

Düşük kohezyonlu killerde konsol istinat yapılarının stabilitesi, zemin ile istinat yapıları arasındaki etkileşim nedeniyle özel geoteknik zorluklarla karakterize edilir. Bu bağlamda, bu makalenin amacı bu zeminlerde duvarlara etki eden aktif toprak basınçlarını sayısal olarak analiz etmektir. Sayısal analiz, PLAXIS 2D yazılımı kullanılarak sonlu elemanlar yöntemi ile gerçekleştirilmiştir. Sayısal modelde, sabit 30° içsel sürtünme açısına ve 4 kPa, 8 kPa ve 12 kPa gibi düşük kohezyon değerlerine sahip, birim ağırlığı (γ = 18 kN/m³) olan killi bir zemin kullanılmıştır. Geometrik etkileri incelemek amacıyla, temel genişliği 0,1H, 0,3H ve 0,5H (H: duvar yüksekliği) olarak değiştirilerek parametrik bir çalışma yapılmıştır. Sonuçlar, temel genişliği ve zemin kohezyonunun göçme şekli üzerinde etkili olduğunu göstermektedir.
Anahtar Kelimeler: *Konsol istinat duvarı; Düşük kohezyonlu zemin; Aktif toprak basıncı; Pekleşen zemin modeli.*

ABSTRACT

The stability of cantilever retaining structures in low-cohesion clays presents special geotechnical challenges due to the interaction between the soil and the retaining structures. In this regard, the objective of this paper is to conduct numerical analysis of active earth pressures on the walls in these soils. Numerical analysis has been conducted through finite element analysis using the PLAXIS 2D software. The numerical model used a clayey soil with a constant internal friction angle of 30° and low cohesion values of 4 kPa, 8 kPa, and 12 kPa, and a unit weight (γ = 18 kN/m^3). In order to study geometric effects, a parametric study was conducted by changing the cantilever heel width to 0.1H, 0.3H, and 0.5H (H: Wall Height). The results illustrate that the heel width and soil cohesion have a significant effect on the failure mechanism.
Keywords: *Cantilever wall; Cohesive-frictional backfill; Active earth pressure; Hardening soil model.*

[1] PhD Candidate, Karadeniz Teknik Üniversitesi, dina-aqra@hotmail.com (Sorumlu yazar)
[2] Prof. Dr., Karadeniz Teknik Üniversitesi, esadoglu@ktu.edu.tr

1. INTRODUCTION

Calculations related to lateral earth pressure problems have been carried out since the early 18th century. However, it was only several decades later that Coulomb (1776) conducted the first major study of earth pressures, taking into account a rigid mass of soil sliding upon a shear surface. Years later, another method of calculation was proposed by Rankine (1857) through a different stress field approach, and both approaches are still popular to date for estimating simple lateral earth pressures. In order to solve more complicated problems based on the theories mentioned above, Shukla et al. (2009) have studied the analytical formulations to compute the total active pressure on retaining walls for cohesive-frictional soils. It was found in their research that the parameters of cohesion and shearing resistance angle greatly affect the critical failure plane inclination and pressure changes. Despite the theoretical basis from the previous researchers, the effect of soil cohesion in combination with the shape of the foundation, in particular, the heel width of cantilever walls, on the mobilized earth pressure requires further numerical investigations (Shukla et al., 2009).

Active pressure coefficient and distribution in a c-ϕ backfill do not depend only on the effective friction angle. Analytical studies have revealed that cohesion, wall friction, wall adhesion, unit weight, depth, and soil arching, among other parameters, affect active pressure in a wall backed by c-ϕ backfill (Tu and Jia, 2014). Tu and Jia (2014) identified the limitations of the existing theoretical methods in their analysis of active earth pressure in c-phi backfills, thereby demonstrating that the earth pressure is inherently non-linear due to soil arching and stress rotation. In addition, it was stressed that soil cohesion plays a critical role in minimizing active pressure (Tu and Jia, 2014). Furthermore, finite-element analyses indicate that active pressure mobilization along a wall height depends on soil behavior and wall distortions at various depths, and that a non-linear soil model outperforms elastic-perfectly plastic models in avoiding numerical instabilities during soil-wall interaction analyses (Elchiti et al., 2017). These findings are of particular relevance for cantilever retaining walls where wall rigidity assumptions are changed by foundation shape and wall flexibility (Elchiti et al., 2017; Bruner and Bartoskewitz, 1992).

Pressure and wall friction forces on the stem and foundation base plate have a major influence on the stability of retaining structures. Fukuoka and Yoshida (1975) showed experimentally that wall friction and interface effects considerably modify the principal stress trajectories and distribution of earth pressures, resulting in solutions different from those provided by classical approaches of Coulomb and Terzaghi. In addition, finite element analyses should be able to model the friction and adhesion laws properly at the stem-soil and base-soil interfaces, especially at the heel and base plate of the foundation, rather than taking into account full bonding, since inappropriate modeling of interfaces will result in considerable error in the evaluation of active earth pressure and resistance to sliding (Fukuoka and Yoshida, 1975). In the case of cantilever walls, changing the foundation heel width affects the base-soil interaction.

The research works regarding the calculation of soil pressure behind retaining walls have become increasingly sophisticated over time, as well as the numerical and analytical modeling taking into account the arching action of cohesive-frictional backfill soils. The recently conducted investigations by Sarfaraz et al. (2023) focused on the issue of the nonlinear stress state of retaining walls during active translation modes (Sarfaraz et al., 2023). In addition, according to the recent finite element analysis performed using PLAXIS 2D software, soil cohesion considerably decreases the area of the failure zones and influences the development of the shear strains, while at the same time proving that the shape

of the critical failure surface depends on the heel width ratio (β) of the foundations (Ayman et al., 2025). Moreover, numerical analyses of flexible cantilever retaining walls with cohesive backfill soils have shown that soil cohesion considerably decreases active earth pressures and changes the position of the thrust load application point (El Yamouni et al., 2024). Nonetheless, the effect of varying heel width ratio and cohesion of the soil on the mobilized active earth pressure in cantilever retaining walls needs further investigation.

Nevertheless, despite all of these advances that have been made in modeling cohesive-frictional backfills, the actual geotechnical consequences of the width of the heel as well as the soil cohesion in the design of cantilever retaining walls are not properly understood. To solve this issue, the objective of this study is to study the influence of heel width ratios (β = 0.1, 0.3, 0.5) and changes in cohesion values (c = 4, 8, 12 kPa) for a constant internal friction angle (ϕ = 30) on the active thrust force developed and the non-linear distribution of lateral pressure in cohesive-frictional backfills. For this purpose, the parametric matrix, which includes 9 cases, was studied to analyze the effects of changes in soil and footing geometrical parameters. Two-dimensional (2D) finite element analyses were performed using PLAXIS 2D software to mobilize the active earth pressure acting on a cantilever retaining wall with cohesive-frictional soil having a height of 5.0 m.

2. NUMERICAL METHODOLOGY

Finite element analysis in two dimensions was carried out using PLAXIS 2D software to analyze the mobilization of active earth pressure for a cantilever retaining wall. As illustrated in the schematic diagram of the retaining wall geometry (Figure 1), the structuer is constructed with a backfill height of 5.0 m (H = 5.0 m). In order to study the influence of the configuration of the foundation and soil parameters, a parametric table of 9 numerical scenarios was established (Table 1). Three different foundation heel width ratios (β = 0.1, 0.3, 0.5) were taken into account, along with three different values of cohesion (c = 4, 8, 12 kPa), and an identical internal friction angle (ϕ = 30).

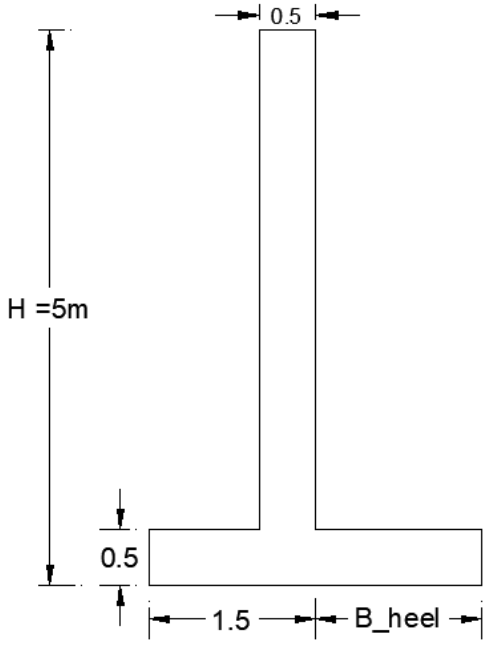

Figure 1. Schematic diagram and geometric dimensions of the analyzed cantilever wall

Table 1. Matrix of Parametric Study

Group	Heel Ratio ($\beta = B_{heel}/H$)	Cohesion	Friction Angle
Cases 1-3	0.1 (0.5m)	Soil 1 (c = 4 kPa)	$\phi = 30^{o}$
		Soil 2 (c = 8 kPa)	
		Soil 3 (c = 12 kPa)	
Cases 4-6	0.3 (1.5m)	Soil 1 (c = 4 kPa)	
		Soil 2 (c = 8 kPa)	
		Soil 3 (c = 12 kPa)	
Cases 7-9	0.5 (2.5m)	Soil 1 (c = 4 kPa)	
		Soil 2 (c = 8 k Pa)	
		Soil 3 (c = 12 kPa)	

The soil backfill material has been considered as a cohesive-frictional soil with the varying value of effective cohesion (c) of 4.0, 8.0, and 12.0 kPa, with a friction angle (ϕ) of 30.0 and a unit weight 18kN/m^3. The Hardening Soil (HS) material (Schanz et al., 1999) has been selected in order to consider the nonlinear stress dependency and shear hardening effects. The reference secant stiffness (E_{50}^{ref}) has been taken as 19.0, 23.0, and 27.0 MPa, corresponding to the cohesion of 4.0, 8.0, and 12.0 kPa. For ensuring mechanical consistency, the reference tangent stiffness for the oedometer test (E_{oed}^{ref}) has been kept equal to E50^ref, while the reference unloading/reloading stiffness (E_{ur}^{ref}) has been taken as three times the reference secant stiffness ($3 \times E_{50}^{ref}$). An interface strength reduction factor (R_{inter}) of 0.60 has also been considered for simulating the interaction between soil and retaining structure. The stress-dependence index m for stiffness was selected as 0.60. Also, the "Tension Cut-off" option was enabled with zero tensile strength (0.0 kN/m²), in order to allow development of the tensile crack depth (zc) in view of the physically impossible sustained tensile stress at the upper fill interface.

The cantilever retaining wall, along with its base slab, was assumed to be a continuous solid element. In order to simulate the mechanical properties of the concrete material, a Linear Elastic material model was used. This is a common practice for soil-structure interaction numerical analyses because the stiffness of the concrete wall is much greater than that of the backfill, and since the main interest of the study is soil yielding processes and not the structural failure of the wall. The concrete material was assumed to be a non-porous drained-type material with a unit weight (γ) of 24.0 kN/m^3. The elastic stiffness parameters included the following: Young's modulus (E) of 30 GPa and Poisson's ratio (ν) of 0.20.

A staged construction analysis procedure was used for the numerical modeling:

1. **Initial Stage & Excavation:** Activation of the retaining wall along with its foundation slab and soil-structure interaction interfaces, followed by the excavation of the soil mass ahead of the wall to establish the initial at-rest stress condition.

2. **Translation Mode (Stages 3 to 19):** Application of a horizontal displacement of the wall to induce an active limit state of equilibrium. This was achieved by increasing the horizontal displacement by 0.001H (0.005 m) in each stage, up to a maximum of 0.017H (0.085 m).

A Vertical Control Section was specified 5 cm behind the retaining wall stem to obtain the lateral stress distribution. The active earth pressure condition is assumed to be mobilized when there is no appreciable change in lateral forces with each displacement increment (approximately 1%).

3. RESULTS AND DISCUSSION

3.1. Mobilization of Active Earth Pressure

Graphical representation of the normalized wall movement (Δx/H) and the total active earth thrust for all nine cases is provided in Figure 2. It is seen that the transition from the at-rest limit state to the active one demonstrates a non-linear tendency, during which there is a considerable reduction of the absolute value of the lateral force in the first stages of the wall displacement process. Curves stabilize themselves, and the change in lateral force approaches zero value, reaching the fully mobilized active limit state.

Moreover, the parametric study allows revealing important behavioral tendencies related to the influence of soil cohesion (c) and heel width ratio (β). As the value of soil cohesion grows, the value of wall displacement necessary for full mobilization of the active earth pressure state also rises. The same tendency takes place if the heel width ratio (β) is reduced. Depending on these parameters, the active state can be achieved at the normalized wall displacement equal to about 0.005 – 0.009.

According to the literature data, the active limit state can usually be achieved with a much smaller displacement in conventional walls. Numerical analysis done by Sarfaraz et al. (2023) shows that the horizontal earth pressure decreases with the movement of the wall and attains constant values at the active wall movement of about 0.0007 times the wall height. This result is also consistent with the results of the previous numerical analysis performed by Matsuzawa and Hazarika (1996), who showed that active wall movement is equal to (Δx/H) = 0.0005 to 0.001 for vertical walls.

It should be noted that in the current investigation, the active state is attained at a larger displacement of Delta x/H = 0.005 to 0.009. The reason behind this apparent delay in the mobilization of the active pressure can be attributed to the effects of both soil cohesion and the heel geometry of the cantilever retaining wall. Soil cohesion creates cohesive bonds, which will have to be sheared and mobilized, while variation in the width of the foundation heel (β) changes the system stiffness and size of shear zones. Hence, a larger movement of the wall is necessary to stretch the cohesive-frictional soil mass to activate it.

3.2. Effect of Heel Width and Soil Cohesion on Active Earth Thrust

It is apparent from Figure 1 that both the heel width ratio (β) and the cohesion of the soil (c) have a vital influence on the magnitude of the mobilized earth thrust force. From the FEA results, at the fully active state (Δx/H = 0.007), the heel width ratio ($\beta = b_{heel}/H$) has a huge influence on the active force.

An increase in the foundation heel width ratio leads to a noticeable increase in the value of the active thrust force. For instance, with a constant soil cohesion of c = 4 kPa, the active force increases from 48.9/m at β = 0.1 to 60.4 kN/m at β = 0.3, and attains 66.8kN/m at β = 0.5. The explanation for this phenomenon lies in the fact that a wider foundation heel engages a larger volume of the cohesive-frictional backfill resting on the heel of the foundation, leading to higher vertical geostatic pressures and structural involvement along the failure plane.

Additionally, an increase in soil cohesion (c) shows an inverse and significant influence on the magnitude of the active force. Comparing the cases with the same heel width ratio of β = 0.5, the active lateral force decreases from 66.8 kN/m for c = 4 kPa, to 54.1 kN/m for c =

8kPa, and achieves its lowest value of 44.9 kN/m for c = 12 kPa due to the enhanced shear resistance provided by the soil cohesion. In general, the maximum active thrust (66.8 kN/m) corresponds to the largest foundation configuration combined with the lowest cohesion (β = 0.5, c = 4 kPa), whereas the minimal active thrust (19.8 kN/m) corresponds to the smallest heel width with higher cohesion (β = 0.1, c = 12kPa). The wider foundation base activates a bigger volume of the cohesive-frictional backfill, shifting the slip surface and altering the lateral driving thrust.

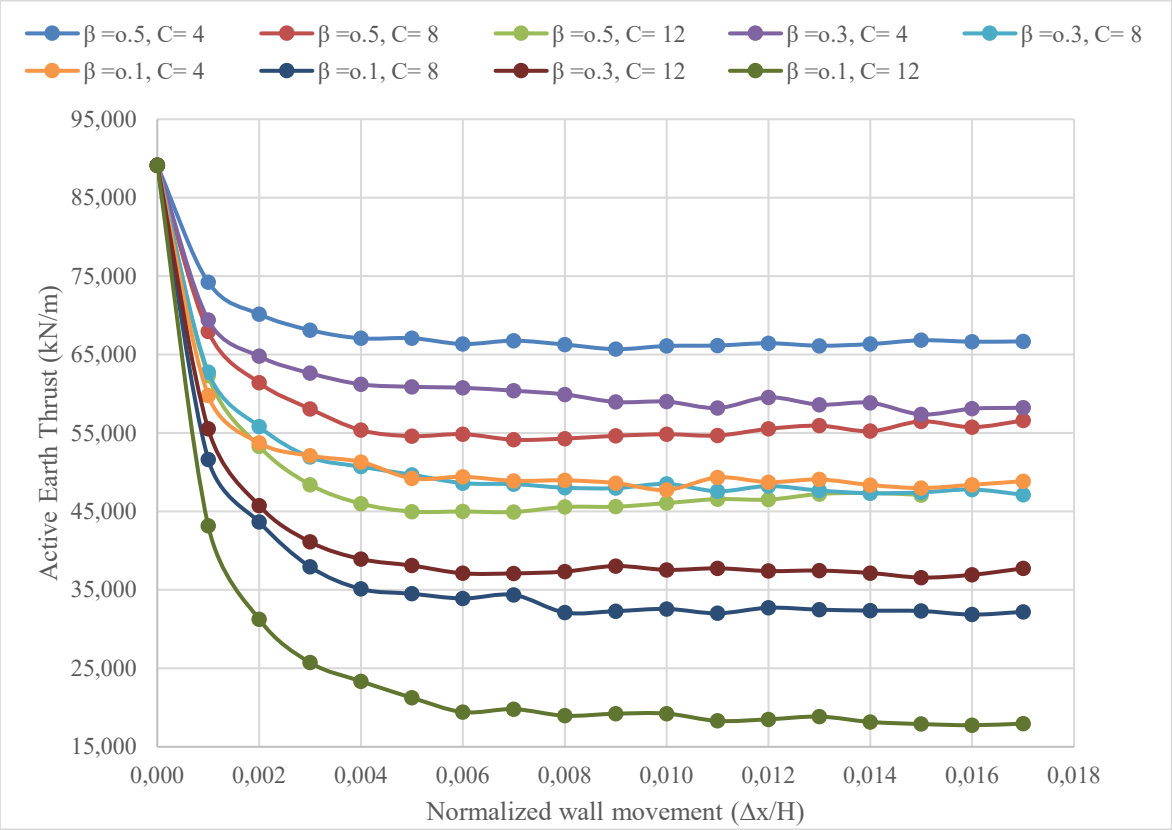

Figure 2. Variation of Active Earth Thrust with Normalized Wall Movement for Different Foundation Heel Widths and Soil Cohesions

This is consistent with very recent and sophisticated numerical studies related to the effect of base geometry on soil kinematics. As classical limit equilibrium analysis assumes a simple failure plane, neglecting complex structural features, the above findings support the complexity of such soil-structure interaction. For example, Ayman et al. (2025) showed that changing the base geometry of a cantilever wall, in particular the heel length at the back, significantly affects the failure process, leading to variations in the volume of mobilization of the cohesive backfill. In the same manner, the current study shows that the width of the foundation heel and soil cohesion have an extremely significant impact, as they affect the principal slip surface and the driving lateral thrust force created as a consequence. This is supported by the work of El Yamouni et al. (2024), as they observed that due to boundary conditions and cohesive-frictional interaction, very nonlinear earth pressures occur which cannot be properly modeled by classical theories.

3.3. Plastic Points and Failure Mechanisms

In the analysis of finite element simulations through the use of the Hardening Soil (HS) model, it becomes necessary to determine the plastic points in space to understand the

yielding and failure characteristics of the backfill. The stresses in PLAXIS 2D models are described using certain plastic point criteria as follows:

- **Hardening points:** The stresses at which the material first comes to the HS model shear yield surface. Before this point, the material response is mainly elastic, though exhibiting non-linear stress-dependent stiffness.
- **Cap points:** Yielding zones under primary volumetric compression.
- **Failure points:** are those zones that have attained the stress state on the yield surface and thus active shear slip zones.
- **Tension cut-off points:** Zones where the stress state exceeds the tensile limit of the cohesive-frictional material, resulting in the formation of tension cracks close to the ground surface.

It was also necessary to carry out the examination of plastic point distributions not only for the mobilized active state ($\Delta x/H = 0.007$) but also beyond the active state. Also, the analysis of failure angles provides evident differences from the geotechnical theory. According to the theories of limit equilibrium and Rankine, the angle of the slip line (θ) should be equal to the theoretical angle of the active failure of $45^\circ + \phi/2$ (60° for $\phi = 30$). But in the calculations, the angles turn out to be less than the theoretical ones. The reason is the cohesion of the soil and the influence of the heel geometry on the actual stress condition.
In addition, the analysis showed that the heel width (β) and the cohesion (c) of the soil exert a significant influence on the behavior of the system. With the increase of the heel width ratio, the kinematics of the failure surfaces alter due to the interaction between the failure surfaces and the tension zones, and the formation of tension cracks on the surface of the ground takes place. Additionally, the extension of the principal slip surface (θ) is affected by the developed tension zones.

Table 2. Measured slip surface angles (Ψ and θ) at active ($\Delta x/H = 0.007$) and post-active ($\Delta x/H = 0.008$) and ($\Delta x/H = 0.009$) stages.

Toe Ratio ($\beta = B_{heel}/H$)	Cohesion	$\Delta x/H = 0.007$		$\Delta x/H = 0.008$		$\Delta x/H = 0.009$	
		Ψ	θ	Ψ	θ	Ψ	θ
0.5	Soil 1 (c=4kPa)	63	49	59	48	59	50
	Soil 2 (c=8kPa)	65	53	58	53	60	55
	Soil 3 (c=12kPa)	57	53	55	50	55	53
0.3	Soil 1 (c=4kPa)	62	55	62	55	60	53
	Soil 2 (c=8kPa)	60	50	63	54	57	54
	Soil 3 (c=12kPa)	60	52	55	49	54	50
0.1	Soil 1 (c=4kPa)	66	52	68	52	68	51
	Soil 2 (c=8kPa)	60	55	58	50	62	52
	Soil 3 (c=12kPa)	63	46	59	48	55	48

The analysis of failure angles shown in Table 2 gives more insight into the kinematics of the backfill. In accordance with Rankine and Coulomb's theory, the active failure angle is theoretically predicted to be constant and equal to $45^\circ + \phi/2$ (60° for $\phi = 30^\circ$). Nevertheless, as can be seen from FEM simulation results, this theoretical prediction is not met due to the significant deviation. At the onset of the active state ($\Delta x/H = 0.007$), the computed primary slip angle θ ranges between 46° and 55°, remaining consistently lower than the theoretical 60°. For instance, with a moderate cohesion of c = 8 kPa, θ is recorded at 53° for $\beta = 0.5$, and adjusts to 50° and 55° for $\beta = 0.3$ and $\beta = 0.1$, respectively. Meanwhile, the secondary failure plane angle Ψ ranges from 55 to 68; specifically, for $\beta = 0.1$ with c = 4 kPa, Ψ reaches 66° at

Δx/H = 0.007, 68 at Δx/H = 0.008, and 68 at Δx/H = 0.009, whereas for β= 0.5 with c = 4 kPa, it equals 63, 59, and 59 accordingly.

Figures 3 to 5 present the plastic point distributions acquired from the finite element analysis at the active and after-active limit states (Δx / H = 0.007, 0.008, and 0.009, for Figures 3, 4, and 5, respectively). Such distributions analyze the intricate relationship between the heel width ratio (β = 0.5, 0.3, 0.1) and different cohesion (c = 4, 8, 12 kPa) on the kinematics of the cohesive-frictional backfill.

The failure points show a clear distinction in the process of formation and movement of both primary and secondary shear slip surfaces, which develop from the heel and toe of the cantilever retaining wall. It can be seen from the plastic point status from Δx/H = 0.007 (Figure 3) to 0.008 and 0.009 (Figures 4 and 5) that there is a continuous process of development of the failure surface during the early stage of translation. By the time the displacement increases to 0.008 and 0.009, there will be a formation of continuous bands of the red markers, which become stable at this point.

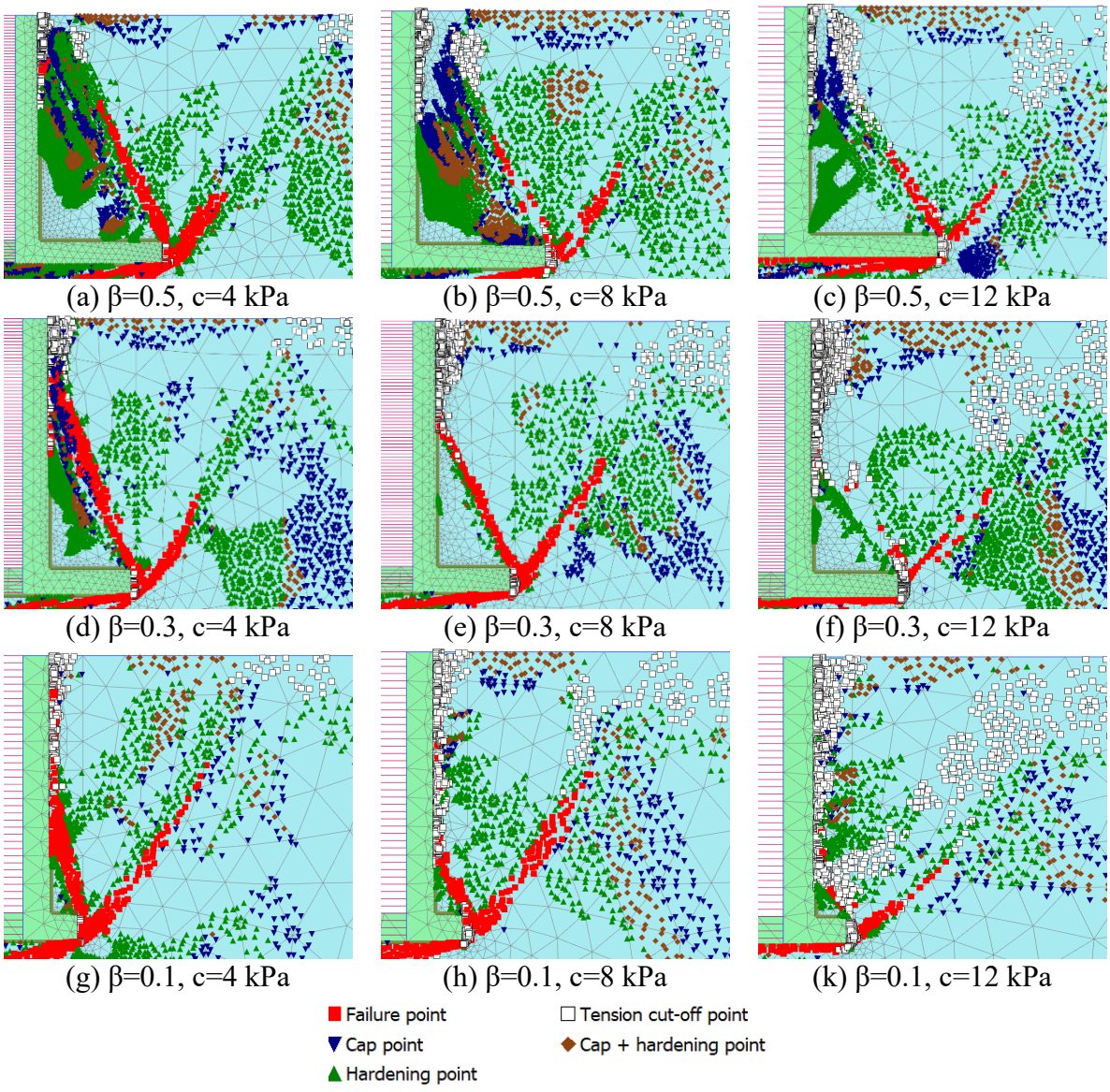

Figure 3. Plastic point distribution illustrating failure surfaces and tension zones across Different Foundation Heel Widths and Soil Cohesions at Δx/H = 0.007 wall movement.

The vertical analysis of the models shows that the geometry of the foundation has an enormous influence on the kinematics of the soil. For the wide foundation (β = 0.5, long heels), the secondary failure angle (Ψ) does not reach the stem of the wall. However, for the narrower heel width ratio of β = 0.3 and 0.1 (smaller heels), the slip surface reaches and penetrates into the upper areas successfully. Instead of continuing to develop freely to the surface, the failure surfaces are stopped when they come into contact with the tensile zone.

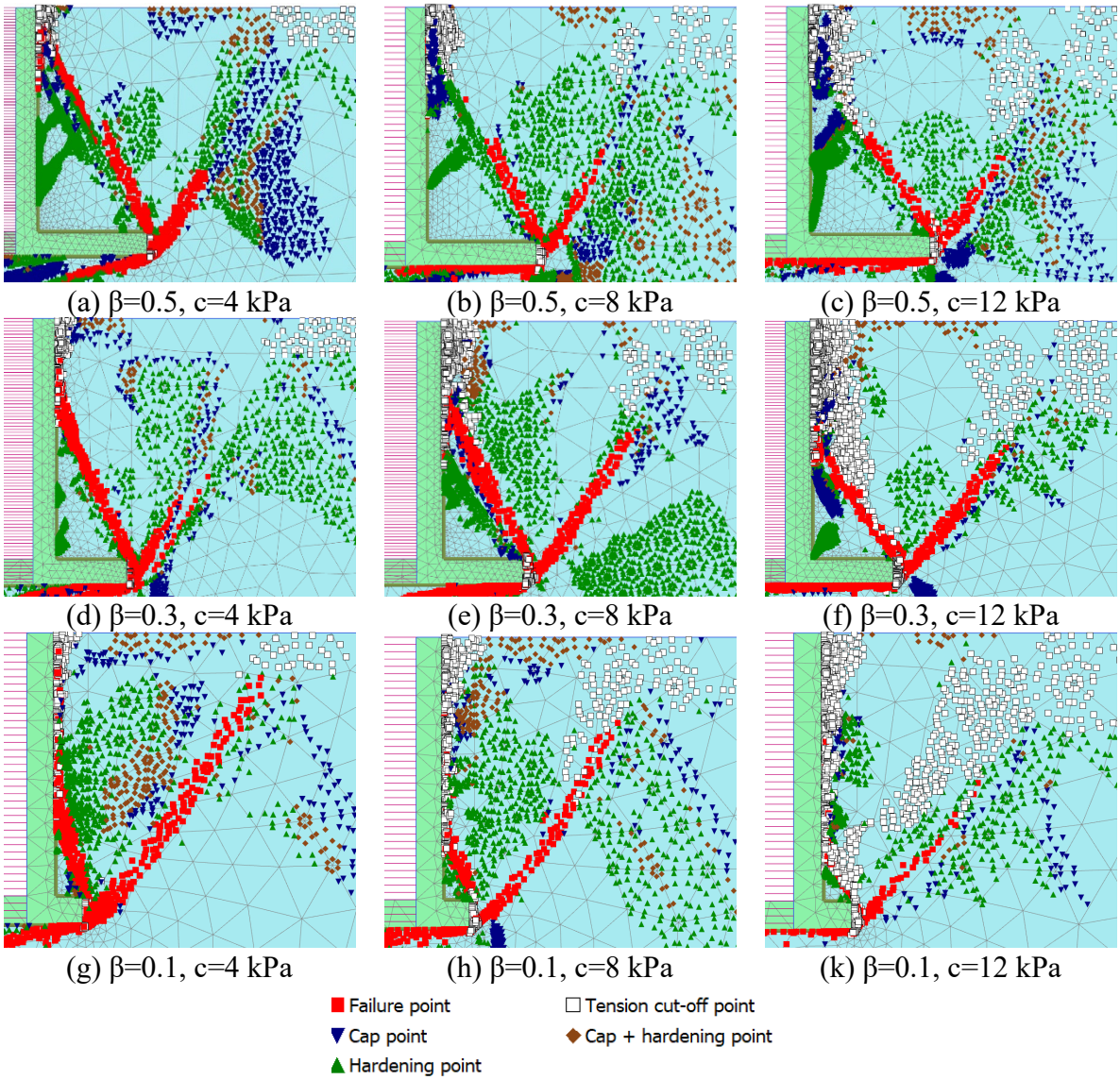

Figure 4. Plastic point distribution illustrating failure surfaces and tension zones across Different Foundation Heel Widths and Soil Cohesions at Δx/H = 0.008 wall movement.

An important point that can be seen about the tension zones (markers in white squares) is their different depths. The depth of the tension zone near the wall stem is noticeably deeper than the depth at which it cuts the main slip plane (θ). This high intensity of the tensile cracks near the wall stem is due to certain boundary conditions and kinematics arising from narrow foundations.

Horizontal examination of the models from left (c = kPa) to right (c = 12 kPa) reveals the fact that a high value of soil cohesion greatly increases the area of the tension cut-off zones on the ground surface behind the retaining wall.

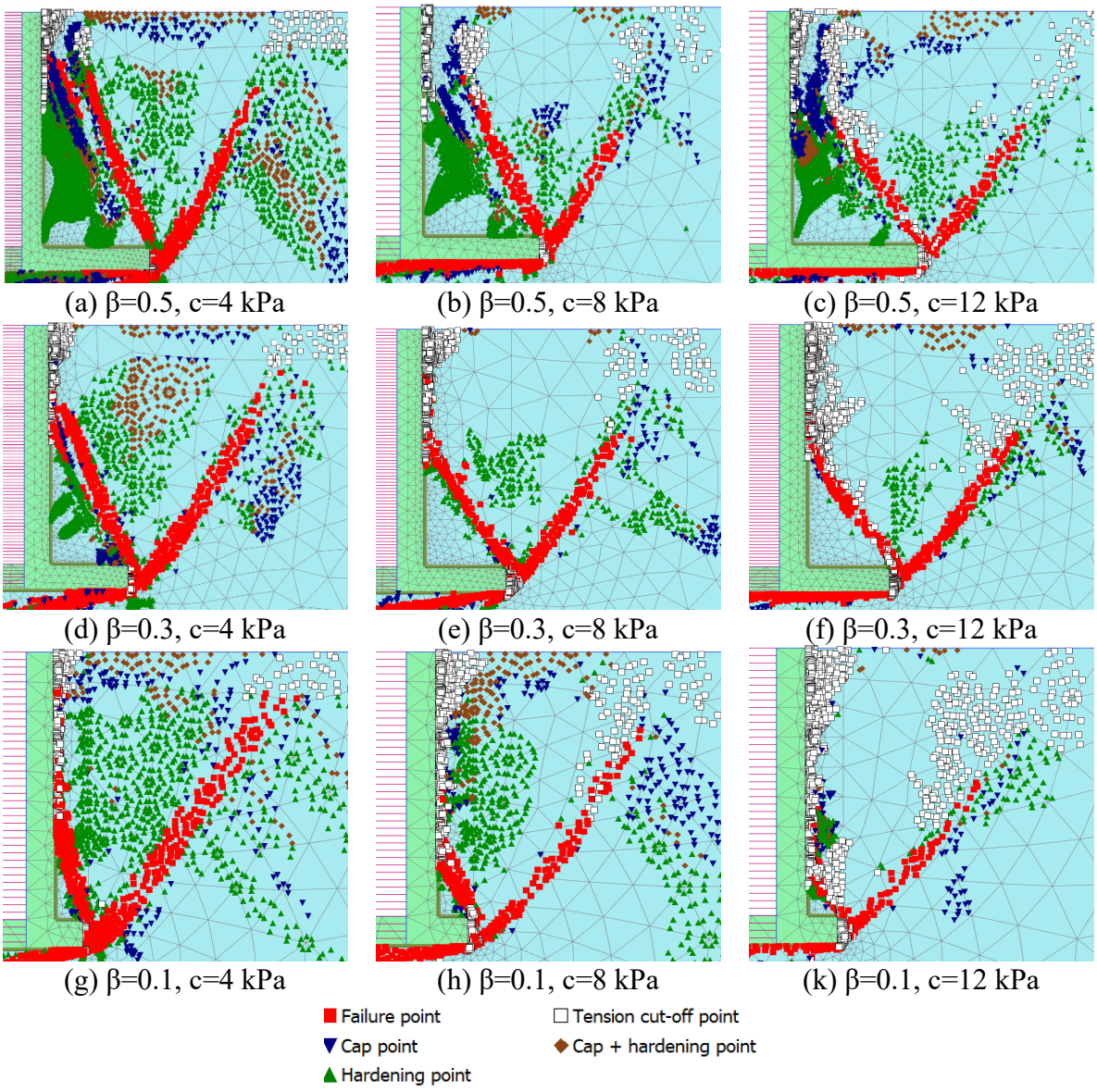

Figure 5. Plastic point distribution illustrating failure surfaces and tension zones across Different Foundation Heel Widths and Soil Cohesions at Δx/H = 0.009 wall movement.

4. CONCLUSİON

This study numerically investigated the effect of the heel width ratio (β = 0.1, 0.3, 0.5) and soil cohesion values (c = 4, 8, 12 kPa, with a constant friction angle ϕ = 30̊) on the active lateral earth pressure exerted on cantilever retaining walls supporting cohesive-frictional backfill. Using PLAXIS 2D and the Hardening Soil constitutive model, nine different parametric configurations have been studied at various displacement stages. The main findings of this analysis are as follows:

• Active Limit State Mobilization: The active limit state is increasingly mobilized by the movement of the wall in the direction of displacement. From the finite element analysis, it can be observed that a lateral displacement of $\Delta x/H$ equal to 0.005 to 0.009 is necessary to mobilize the shear resistance of the cohesive-frictional backfill.

• Effect of foundation heel width (β) and soil cohesion: The active lateral force is largely dependent on the relative width (β) and the soil cohesion. An increase in the width ratio ($\beta = 0.5$) is known to lead to an increase in the active earth thrust. At a constant soil cohesion of $c = 4$, when β changes from 0.3 to 0.5, the active force increases from 60.4 kN/m to 66.8 kN/m. However, an increase in cohesion will result in a decrease in active lateral pressure. At a constant width ratio ($\beta = 0.5$), when soil cohesion changes from 4 to 8, the active force decreased from 66.8 kN/m to 54.2 kN/m.

• Failure Modes & Plastic Points: The failure mechanisms and the locations of plastic points, when examined in terms of the plastic points and failure angles, show that the presence of soil cohesion and varying foundation heel width (β) leads to noticeable departures from classical Rankine and Coulomb theories ($45 + \phi/2$).

REFERENCES

Coulomb, C. A. (1776), “Essai sur une application des règles de maximis et minimis à quelques problèmes de statique, relatifs à l'architecture”, Mémoires de Mathématique et de Physique, Vol 7, 343–382.

Rankine, W. J. M. (1857), “On the stability of loose earth”, Philosophical Transactions of the Royal Society of London, Vol 147, 9–27.

Shukla, S. K., Gupta, S. K. and Sivakugan, N. (2009), “Active earth pressure on retaining wall for c-ϕ soil backfill under seismic loading condition”, Journal of Geotechnical and Geoenvironmental Engineering, Vol 135(5), 690–696.

Tu, B. and Jia, J. (2014), “Active earth pressure from c-φ soil backfill”, Proceedings of the Institution of Civil Engineers - Geotechnical Engineering, Vol 167(6), 548-559.

Elchiti, I., Saad, G., Najjar, S. and Nasreddine, N. (2017), “Investigation of active soil pressures on retaining walls using finite element analyses”, Geotechnical Frontiers 2017, 153-162, American Society of Civil Engineers.

Bruner, R. F. and Bartoskewitz, R. E. (1992), “Cantilever retaining wall design”, Research Report 236-2F, Texas Transportation Institute, Texas A&M University System.

Fukuoka, M. and Yoshida, Y. (1975), “Researches on earth pressure about cantilever wall with cohesive soil as backfill”, International Journal of Rock Mechanics and Mining Sciences & Geomechanics Abstracts, Vol 16(2), 52-53.

Sarfaraz, H., Khosravi, M. H. and Pipatpongsa, T. (2023), “Theoretical and Numerical Analysis of Cohesive-Frictional Backfill against Battered Retaining Wall under Active Translation Mode”, International Journal of Geomechanics, Vol 23(6).

Ayman, G., El Khannoussi, F., El Yamouni, B. and Khamlichi, A. (2025), “Analysis of seismic dynamic thrust for cantilever retaining walls as affected by sloped backfill and

surcharge: from finite element modeling to simplified sliding surface geometry", Journal of Engineering and Applied Science, Vol 72(160).

El Yamouni, B., El Khannoussi, F. and Khamlichi, A. (2024), "Numerical Investigation of Seismic Behaviour for a Flexible Cantilever Retaining Wall with Cohesive Backfill", International Journal of Engineering Research in Africa, Vol 69, 125–142.

Schanz, T., Vermeer, P. A. and Bonnier, P. G. (1999), "The hardening soil model: Formulation and verification", Beyond 2000 in Computational Geotechnics, 281–296, Routledge, London.

SYMBOL LİST

Symbol	Explanation	Symbol	Explanation
c	**Cohesion of the soil (kPa)**	**ϕ**	**Internal friction angle of the soil**
γ	**Unit weight of the material (kN/m^3)**	**H**	**Height of the retaining wall (m)**
Δx	**Horizontal displacement of the retaining wall**	**Δx/H**	**Normalized wall movement**
β	**Foundation heel width ratio**	E_{50}^{ref}	**Reference secant stiffness from drained triaxial tests**
E_{oed}^{ref}	**Reference tangent stiffness for primary oedometer loading**	E_{ur}^{ref}	**Reference unloading/reloading stiffness**
R_{inter}	**Interface strength reduction factor**	**ν**	**Poisson's ratio**